

Photoacoustic/ultrasound dual modality imaging aided by acoustic reflectors

Guangjie Zhang (张广杰)^{1,2}, Yu Sun (孙宇)^{1,2}, Xing Long (龙星)^{1,2}, Rui Zhang (张睿)³, Meng Yang (杨萌)^{3*}, and Changhui Li (李长辉)^{2**}

¹Department of Biomedical Engineering, College of Engineering, Peking University, Beijing 100871, China

²College of Future Technology, Peking University, Beijing 100871, China

³Ultrasonography, Peking Union Medical College Hospital, Chinese Academy of Medical Sciences & Peking Union Medical College, Beijing 100730, China

*Corresponding author: amengameng@hotmail.com

**Corresponding author: chli@pku.edu.cn

Received May 17, 2021 | Accepted June 19, 2021 | Posted Online September 15, 2021

Photoacoustic imaging (PAI) with a handheld linear ultrasound (US) probe is widely used owing to its convenient and inherent dual modality capability. However, the limited length of the linear probe makes PAI suffer from the limited view. In this study, we present a simple method to substantially increase the view angle aided by two US reflectors. Both phantom and *in vivo* animal study results have demonstrated that the imaging quality can be greatly improved with the reflector without sacrificing the imaging speed.

Keywords: photoacoustic imaging; limited view; multimodal imaging.

DOI: [10.3788/COL202119.121702](https://doi.org/10.3788/COL202119.121702)

1. Introduction

Photoacoustic (PA) imaging (PAI) uniquely combines the optical absorption contrast with ultrasound (US) detection. Owing to the much weaker US scattering by soft tissue than optical scattering, PAI has successfully broken the barrier in the imaging depth of high-resolution optical imaging^[1–3]. Over past decades, PAI has been widely used in pre-clinical studies and is under rapid pace into clinical implementations^[4–7]. Among various PAI systems, the linear handheld probe-based system is one of the most commonly used, which is not only because of its simplicity and convenience, but also for its inherent capability to perform US imaging simultaneously. Therefore, PA/US dual modality with a linear handheld probe gained much attention in both research and clinical studies^[8–12].

In general, the quality of the PA image reconstruction increases with more PA signals acquired from a wider view angle. However, the short length of the probe strictly limits the view of the handheld probe. For instance, a typical clinical handheld probe is about 4 cm long, so the maximum acquisition angle for a central target at the 2 cm depth under the probe is 45 deg. The limited view not only causes image artefacts, but also leads to failure in reconstruction of features due to the unavailability to detect PA signals out of the view^[13]. Several methods have been explored to alleviate this problem.

Scanning the linear probe over the imaged target (or equivalently rotating the target) is one of the easy ways to increase the view angle, at the expense of longer imaging time. Sophisticated reconstruction algorithms have also been developed to suppress the image artefacts and improve the overall quality^[14–16]. More recently, several methods employ artificial intelligence (AI), especially deep learning, to help the PA image reconstruction^[17,18]. But, those studies based on advanced reconstruction algorithms are not good at recovering lost features due to the lack of PA signals in the out of view region.

Acoustic waves can be reflected at the boundary like other waves, so the acoustic reflector can redirect the undetected PA signal back to the linear probe. Therefore, several previously reported works discussed this way to compensate the limited view^[19–22]. However, only phantom and simple thin tissues have been imaged, and no studies of imaging complicated deep living tissues, such as the trunk of the mouse, have been reported. In this work, we developed an imaging system with two acoustic reflectors that can increase the total view angle to almost 180 deg. Besides, the system also performs simultaneous US imaging, achieving dual modal imaging. In addition to phantom study, we also imaged an *in vivo* animal body. Our results demonstrated that acoustic reflectors can substantially help linear handheld probe-based PAI to retrieve lost features and improve the imaging quality.

2. Experimental Setup and Results

The imaging system is presented in Fig. 1(a), where the acoustic reflector setup is composed of two right angle prisms with a width of 5 cm and a length of 10 cm. Two prisms were closely contacted, and their hypotenuse surfaces serve as two US reflectors. To support the imaged target, part of the “V-shape” dip between the two reflectors is filled with a transparent agarose platform, which is both acoustically and optically transparent. The real US probe with two mirror virtual probes is shown in Fig. 1(b). The overall system design is similar to the previously reported work^[22], while we used two acoustic reflectors at 45 deg instead of 30 deg. To accurately locate the surface location, we marked a series of black dots along the straight line onto the two surfaces of the reflectors, which can be easily reconstructed. The PA image was reconstructed by a filtered back-projection algorithm^[23].

A clinical US system (Resona7, Mindray Bio-Medical Electronics, Shenzhen, China), which is connected to a 192-element linear probe with a central frequency of about 5 MHz, was modified to perform US/PA dual modality imaging. The laser source is an optical parameter oscillation (OPO) laser (SpitLight EVO 200, InnoLas Laser GmbH, Krailling, Germany) with a repetition rate of 10 Hz. In our study, 750 nm was used for PAI with pulse energy of 50 mJ, and the fluence rate onto the tissue body is less than 10 mJ/cm². More details of the PA/US system are described in Ref. [10]. The laser was delivered via a one-two fiber bundle, and the two bundle terminals were mounted on two sides of the acoustic reflectors to illuminate the target.

We first did a phantom imaging study. Two carbon rods with a diameter of 0.3 mm were glued to form a cross and buried in an optically scattering wax phantom, which is composed of gel wax and TiO₂^[24]. Figure 2 shows the dual modality imaging setup and results of the phantom study, in which Fig. 2(a) is the schematic of the setup, and a photograph is provided in Fig. 2(b). Two fused results were presented in Figs. 2(c) and 2(d) for PA image reconstruction without and with two US reflectors, respectively.

As shown in Fig. 2(c), only the horizontal rod is effectively reconstructed, while the vertical rod is missing due to the lack of PA signals from the vertical rod, which predominately traveled along the horizontal direction. However, after using the virtual probes, those missed signals were retrieved, and the cross

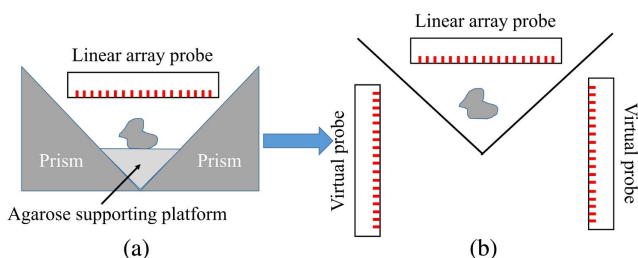


Fig. 1. Schematic mechanism of acoustic reflectors for PAI. (a) System setup; (b) the original probe has two virtual probes corresponding to two reflectors.

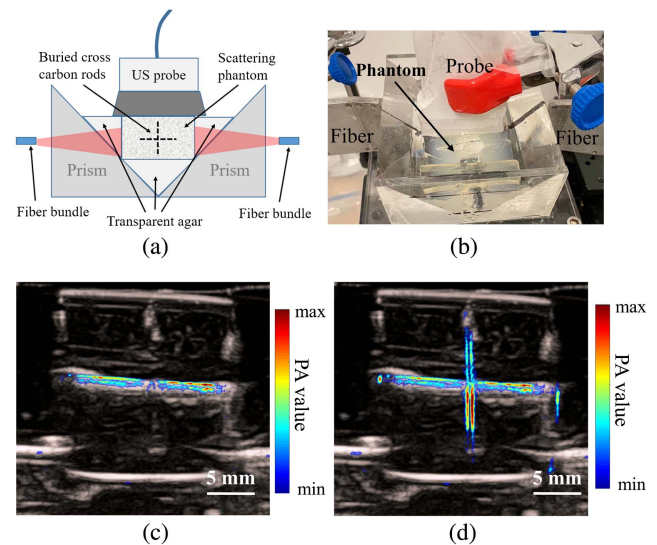


Fig. 2. Phantom experiment. (a) The schematic of the imaging setup; (b) a photograph of the imaging setup; (c) and (d) PA results without and with reflectors, respectively.

was completely reconstructed, as shown in Fig. 2(d). Our phantom result is consistent with previously reported results. The “split” pattern in reconstructed PA images is caused by the limited bandwidth of the clinical US probe.

Then, we did *in vivo* imaging of a BALB/C nude mouse of 19 g, which was anesthetized by intraperitoneal injection with Avertin at 2.5 mg/10 g. Figure 3(a) is the schematic of the imaging setup, in which we first inserted the mouse into a “U-shape” groove in an agarose phantom, so the mouse bottom and two sides closely touched the phantom, then US coupling gel was applied on top of the mouse to fill any air gaps, and another

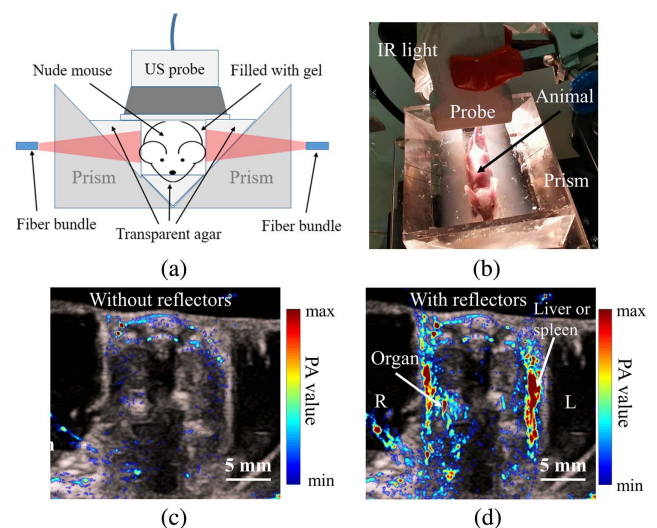


Fig. 3. *In vivo* animal experiment. (a) The schematic of the imaging setup; (b) a photograph of the imaging setup; (c) and (d) fused PA/US results reconstructed without and with two reflectors, respectively. L, left; R, right.

transparent gel pad was put on top of the gel. To keep the mouse body temperature, an infrared (IR) light shone onto the mouse during the experiment, as shown in Fig. 3(b). All animal procedures complied with protocols approved by the Institutional Animal Care and Use Committee of Peking University.

Compared with Fig. 3(c), the reconstructed result with PA signals reflected by two reflectors contains many more features, as shown in Fig. 3(d). It is obvious that one large region on the left (marked as L) of the mouse has a strong PA value after using PA signals from the reflectors. We suspected this region is part of the liver or spleen after comparing with that previously reported in Ref. [25], in which the outer layer of both the liver and spleen generated strong PA signal (due to the blood rich characteristic). Because the mouse in this experiment is closely “packed” in the “U-shape” groove, the liver or spleen organ boundary becomes vertically flattened. In addition, an “organ-like” feature on the right side of the mouse is co-registered with more PA reconstructed features. Unfortunately, we only had access to a clinical US probe aimed for breast imaging in this study, whose spatial resolution is not suitable for small mouse study. So, it was hard for us to distinguish and tell the organ type.

3. Discussion and Summary

In this study, we demonstrated that the acoustic reflector can help PA image reconstruction of complicated deep living tissues. According to our phantom and *in vivo* animal study results, the acoustic reflector is a simple way to effectively retrieve those lost PA signals that cannot be detected by a traditional linear probe and thus substantially improve the PA image reconstruction. It is worth noting that the US reflector could not only help PAI, but also help US imaging itself, since the mirrored US images also exist. Since PA signals reflected from the acoustic reflector may undergo a round-trip through the animal body, the difference in the sound speed between the tissue and surrounding medium could cause image artefact, which needs more studies. In addition, as discussed in Ref. [22], this study neglected the complexity of considering the amplitude and phase change via reflection. We would replace the glass reflector with a thin membrane, forming a water/air boundary to guarantee total reflection without phase change in the future. Other future system improvements include the replacement of the US probe with a wider bandwidth to increase the spatial resolution and the optimization of the illumination design to achieve a more uniform PA excitation, such as a multi-angle ring illumination mode. Finally, the proposed method also has clinical implementation potentials, including PAI of fingers, arms, and legs.

Acknowledgement

This work was supported by the National Key Research and Development Program (Nos. 2017YFE0104200 and 2017YFC0907604), the National Natural Science Foundation of China (Nos. 81421004 and 81301268), the National Key Instrumentation Development Project (No. 2013YQ030651),

the Beijing Natural Science Foundation (No. JQ18023), Beijing Nova Program Interdisciplinary Cooperation Project (No. xxjc201812), and International S&T Cooperation Program of China (No. 2015DFA30440).

References

1. S. Zackrisson, S. van de Ven, and S. S. Gambhir, “Light in and sound out: emerging translational strategies for photoacoustic imaging,” *Cancer Res.* **74**, 979 (2014).
2. P. Beard, “Biomedical photoacoustic imaging,” *Interf. Focus* **1**, 602 (2011).
3. C. Li and L. V. Wang, “Photoacoustic tomography and sensing in biomedicine,” *Phys. Med. Biol.* **54**, R59 (2009).
4. Y. Zhou, J. Yao, and L. V. Wang, “Tutorial on photoacoustic tomography,” *J. Biomed. Opt.* **21**, 061007 (2016).
5. T. Feng, Y. Zhu, Y. Xie, D. Ta, J. Yuan, and Q. Cheng, “Feasibility study for bone health assessment based on photoacoustic imaging method,” *Chin. Opt. Lett.* **18**, 121704 (2020).
6. X. Wang and S. Yang, “Imaging of human wrist joint by a flexible-transducer-based morphological-adaptive photoacoustic tomography: a feasibility study,” *Chin. Opt. Lett.* **17**, 091701 (2019).
7. L. V. Wang and S. Hu, “Photoacoustic tomography: *in vivo* imaging from organelles to organs,” *Science* **335**, 1458 (2012).
8. M. C. Li, C. B. Liu, X. J. Gong, R. Q. Zheng, Y. Y. Bai, M. Y. Xing, X. M. Du, X. Y. Liu, J. Zeng, R. Q. Lin, H. C. Zhou, S. J. Wang, G. M. Lu, W. Zhu, C. H. Fang, and L. Song, “Linear array-based real-time photoacoustic imaging system with a compact coaxial excitation handheld probe for non-invasive sentinel lymph node mapping,” *Biomed. Opt. Express* **9**, 1408 (2018).
9. Y. Y. Bai, B. Cong, X. J. Gong, L. Song, and C. B. Liu, “Compact and low-cost handheld quasibright-field linear-array probe design in photoacoustic computed tomography,” *J. Biomed. Opt.* **23**, 121606 (2018).
10. M. Yang, L. Zhao, F. Yang, M. Wang, N. Su, C. Zhao, Y. Gui, Y. Wei, R. Zhang, J. Li, T. Han, X. He, L. Zhu, H. Wu, C. Li, and Y. Jiang, “Quantitative analysis of breast tumours aided by three-dimensional photoacoustic/ultrasound functional imaging,” *Sci. Rep.* **10**, 8047 (2020).
11. I. Ivankovic, E. Mercep, C. G. Schmedt, X. L. Dean-Ben, and D. Razansky, “Real-time volumetric assessment of the human carotid artery: handheld multispectral photoacoustic tomography,” *Radiology* **291**, 45 (2019).
12. F. Knieling, C. Neufert, A. Hartmann, J. Claussen, A. Ulrich, C. Egger, M. Vetter, S. Fischer, L. Pfeifer, A. Hagel, C. Kielisch, R. S. Görtz, D. Wildner, M. Engel, J. Röther, W. Uter, J. Siebler, R. Atreya, W. Rascher, D. Strobel, M. F. Neurath, and M. J. Waldner, “Multispectral photoacoustic tomography for assessment of Crohn’s disease activity,” *New Eng. J. Med.* **376**, 1292 (2017).
13. Y. Xu, L. V. Wang, G. Ambartsoumian, and P. Kuchment, “Reconstructions in limited-view thermoacoustic tomography,” *Med. Phys.* **31**, 724 (2004).
14. C. Tao and X. J. Liu, “Reconstruction of high quality photoacoustic tomography with a limited-view scanning,” *Opt. Express* **18**, 2760 (2010).
15. X. Lin, N. Feng, Y. Qu, D. Chen, Y. Shen, and M. Sun, “Compressed sensing in synthetic aperture photoacoustic tomography based on a linear-array ultrasound transducer,” *Chin. Opt. Lett.* **15**, 101102 (2017).
16. J. Meng, C. Liu, J. Kim, C. Kim, and L. Song, “Compressed sensing with a Gaussian scale mixture model for limited view photoacoustic computed tomography *in vivo*,” *Technol. Cancer Res. Treat.* **17**, 1 (2018).
17. K. H. Jin, M. T. McCann, E. Froustey, and M. Unser, “Deep convolutional neural network for inverse problems in imaging,” *IEEE Trans. Image Process.* **26**, 4509 (2017).
18. S. Guan, A. A. Khan, S. Sikdar, and P. V. Chitnis, “Limited-view and sparse photoacoustic tomography for neuroimaging with deep learning,” *Sci. Rep.* **10**, 8510 (2020).
19. B. T. Cox, S. R. Arridge, and P. C. Beard, “Photoacoustic tomography with a limited-aperture planar sensor and a reverberant cavity,” *Inverse Probl.* **23**, S95 (2007).
20. R. Ellwood, E. Zhang, P. Beard, and B. Cox, “Photoacoustic imaging using acoustic reflectors to enhance planar arrays,” *J. Biomed. Opt.* **19**, 126012 (2014).

21. B. Huang, J. Xia, K. Maslov, and L. Wang, "Improving limited-view photoacoustic tomography with an acoustic reflector," *J. Biomed. Opt.* **18**, 110505 (2013).
22. G. Li, J. Xia, K. Wang, K. Maslov, M. A. Anastasio, and L. V. Wang, "Tripling the detection view of high-frequency linear-array-based photoacoustic computed tomography by using two planar acoustic reflectors," *Quant. Imaging Med. Surg.* **5**, 57 (2014).
23. M. Xu and L. V. Wang, "Universal back-projection algorithm for photoacoustic computed tomography," *Phys. Rev. E* **71**, 016706 (2005).
24. E. Maneas, W. Xia, O. Ogunlade, M. Fonseca, D. I. Nikitichev, A. L. David, S. J. West, S. Ourselin, J. C. Hebden, T. Vercauteren, and A. E. Desjardins, "Gel wax-based tissue-mimicking phantoms for multispectral photoacoustic imaging," *Biomed. Opt. Express* **9**, 1151 (2018).
25. L. Li, L. Zhu, C. Ma, L. Lin, J. Yao, L. Wang, K. Maslov, R. Zhang, W. Chen, J. Shi, and L. V. Wang, "Single-impulse panoramic photoacoustic computed tomography of small-animal whole-body dynamics at high spatiotemporal resolution," *Nat. Biomed. Eng.* **1**, 0071 (2017).